

# The influence of the torsional restraint of crane column brackets on their critical load capacity

Michał Redecki<sup>1,\*</sup> and Bronisław Gosowski<sup>2</sup>

<sup>1</sup>Wrocław University of Science and Technology, Faculty of Civil Engineering, Department of Metal Structures, Wybrzeże Wyspiańskiego 27, 50-370 Wrocław

<sup>2</sup>Wrocław University of Environmental and Life Sciences, Faculty of Environmental Engineering and Geodesy, Institute of Building Engineering, ul. Norwida 25, 50-375 Wrocław, Poland

**Abstract.** The paper presents the results of numerical parametric studies conducted on laterally restrained steel I-columns with a single stepped asymmetric change in their cross-section. Such elements are used as a part of the outermost columns in the transversal system of steel halls with cranes. The columns are usually braced along their length with wall girts, which in a properly structured hall system have a significant effect on the columns' load bearing capacity and determine their axis of rotation. The main aim of the presented studies is to determine the impact of parameters, such as longitudinal load distribution on the upper and lower segment of the column, the number of pointed lateral bracings and their distance to a column's external flange, and also the application of torsional restraint on the critical load capacity. Results are presented as surfaces or contour maps, in which the ordinates represent the critical loads with regards to the analysed parameters. The paper ends with practical conclusions.

## 1 Introduction

The paper presents the results of an extensive numerical parametric investigation conducted on laterally restrained steel I-columns with a single step asymmetric change in their cross section. In practice, such columns are used as the outermost columns in the non-sway transverse systems of steel industrial halls with cranes. The columns are usually braced along their length with wall girts, which in a properly structured hall system have a significant effect on the columns' load bearing capacity and determine their axis of rotation. By taking into consideration additional stiffeners as torsional

restraint located on the bracket, it is possible to significantly increase its critical load capacity between the lower and upper part of the column.

Undertaken assumption that such systems may be considered as non-sway frames is fully justified. Steel transverse systems not only should fulfill ultimate limit state conditions but also serviceability state conditions. The second ones are much more strict in a reference to horizontal displacements of columns at crane support level. Thus such limitation may be resolved by designing a longitudinal roof bracing system. This solution in accordance with vertical bracings in the plane of gable walls imposes the non-sway mode.

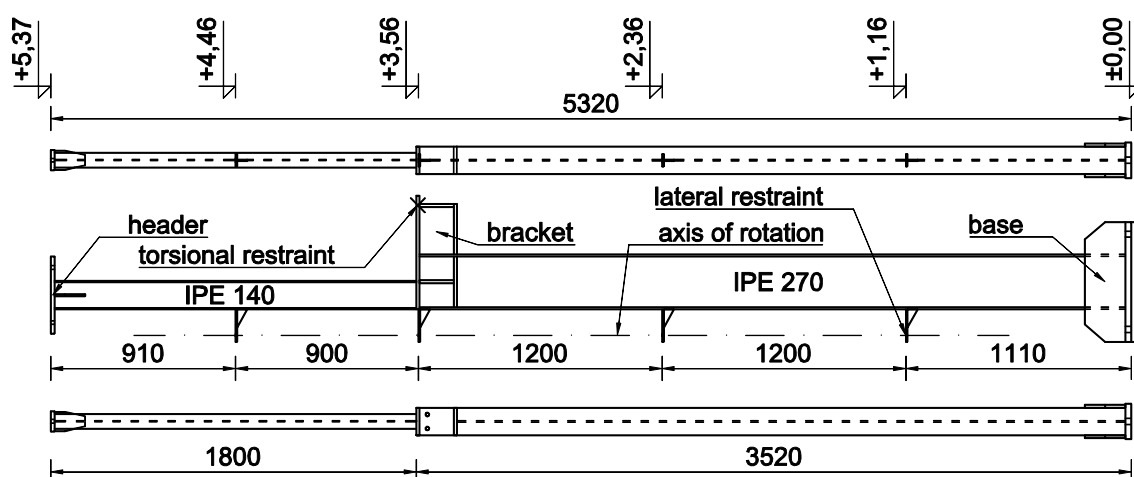
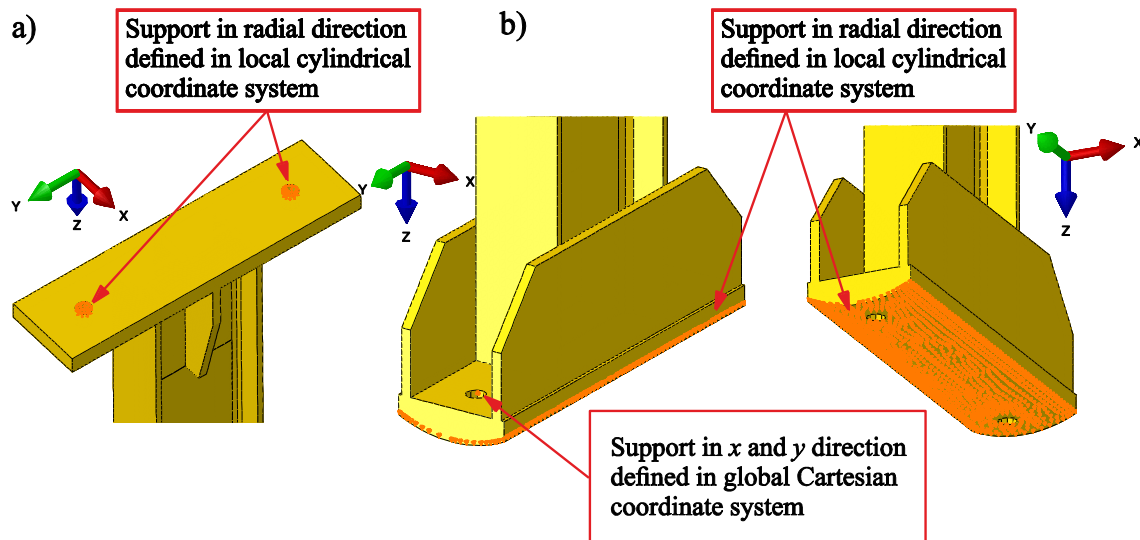


Fig. 1. General view on examined stepped column.

\* Corresponding author: [michal.redecki@pwr.edu.pl](mailto:michal.redecki@pwr.edu.pl)



**Fig. 2.** Details of the header (a) and the base of the investigated model (b).

Spatial stability issues, such as flexural-torsional buckling or buckling along the prescribed axis of rotation, are very relevant from the designing point of view due to precise characterisation of the computational model allowing these kind of structures to be designed more efficiently. Some basic guidelines related to the shaping and designing of stepped columns in industrial buildings can be found in [1-2]. At the stage of verifying structural elements, determination of their critical loads is also required. The majority of available literature only refers to very well examined flexural-buckling [3-4]. More complex examples of flexural torsional buckling of laterally restrained I-sections are presented, among others, in [5-6], and with reference to elements with stepped change of their sectional stiffness, in [7-8].

The numerical investigation is part of a wider study [9], and not only consists of the parametric analysis presented in the current article, but also refers to the experimental and theoretical approach.

## 2 Numerical models

The numerical investigation was conducted on a set of computational models made of two I-sections. The dimensions and shapes of the cross-sections were selected according to the previously mentioned experimental investigation [9]. The lower part of the column is made of IPE 270 profile and the upper part of IPE 140. The total height of the column is 5.32 m. The ratio between the height of the upper and lower segments is around 1:2, which means that they are made in a semi-industrial scale. Both profiles are joined together and their external flanges are in one plane. An example of one of the elements under investigation is shown in Figure 1.

Numerical computations were carried out with the use of the Abaqus FEA package [10] – software commonly used in scientific simulations. Access to both the software and High Performance Computing Services is supported by Wrocław Centre for Networking and Supercomputing.

C3D20R finite solid elements, available in the software library, were used to build the model. The behaviour of the material is described by using Hook's isotropic relationship with Young's elastic modulus  $E$  equal to 194 kN/mm<sup>2</sup> and Poisson's ratio equal to 0.3. The material characteristics come from tensile tests of specimens taken from physical models [9]. The values of critical buckling loads  $N_{cr}$  were obtained by using linear buckling analysis (LBA). This procedure was implemented in the software as the *buckle* in the *linear perturbation* option, which is a part of the *Standard* module.

The numerical model was supposed to describe the real behaviour of the examined element. Moreover, such a structure is very sensitive to any changes of boundary conditions, which is why the support conditions in physical and numerical models should be equivalent. These are defined in a similar way for the whole set of numerical models. The bottom surface of the physical model base plate is rounded (to map a roller bearing) and anchored to the foundation by two M20 bolts (to map a completely fixed support). The main reason for such a solution was to obtain a hinge in a weaker axis and a fixed support in a stronger axis of the cross-section. Its numerical equivalent is shown in Figure 2b. Figure 2a presents the header of the column. In the real element, it was impossible to construct the ideal joint, which is why we can treat this junction as a semi-rigid connection. For

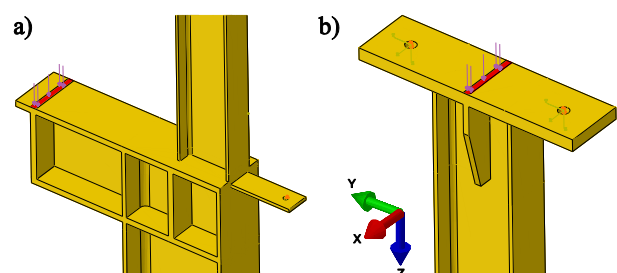


**Fig. 3.** Details of the application of loads to the model in the case of bracket  $N_d$  (a) and header  $N_g$  (b).

**Table 1.** The convention of naming computational models in parametric studies.

Type of support	Bracket torsional restraint	Number of lateral restraints of the upper $m_g$ and lower $m_d$ segment				
		$m_g = 0$ $m_d = 1$	$m_g = 1$ $m_d = 2$	$m_g = 2$ $m_d = 3$	$m_g = 3$ $m_d = 4$	$m_g = 0$ $m_d = 0$
Roller bearing	no	00xx	10xx	20xx	30xx	40xx
	yes	01xx	11xx	21xx	31xx	41xx

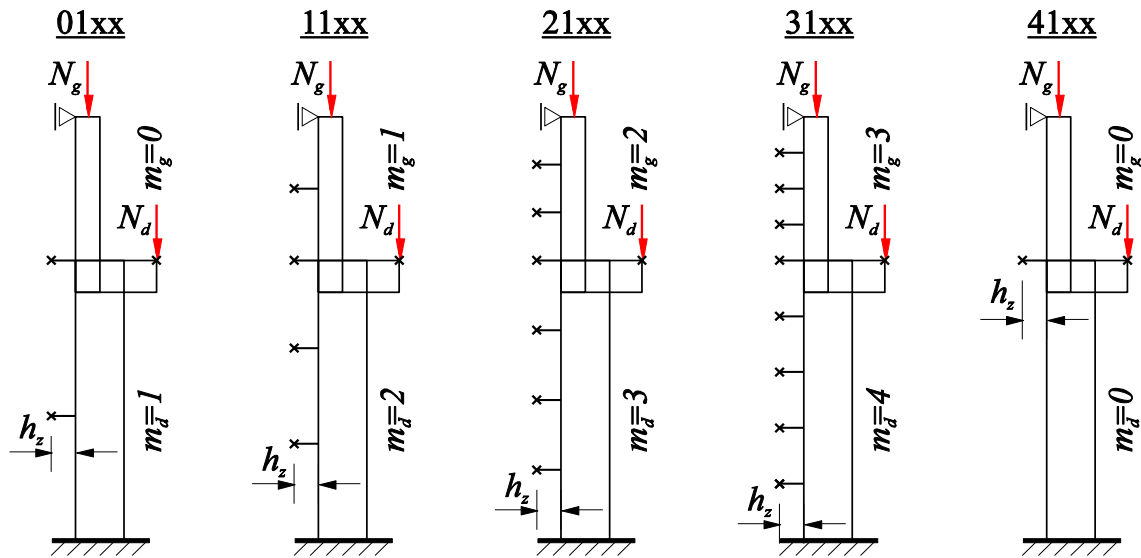


**Fig. 4.** Outlines of the numerical model series x1xx-xxx (with torsional restraint of the bracket).

this purpose, two M16 bolts were used. The bolts in the header were modelled as kinematic constraints defined in a local cylindrical coordinate system located in the middle of the bolt's hole that blocks displacements along its polar coordinates. A similar approach was applied to lateral restraints, which can be observed in Figure 3a, and also to the lower surface of the base plate (see Fig. 2b). Additionally, in this case, to model the vertical support of the whole structure, the local cylindrical coordinate system was covered with the centre of the cylinder from which the base plate was made. Torsional restraints were modelled in a global coordinate system as lateral supports applied to the top flange of the bracket near the area where loads had been applied.

Actions were applied to the structure on its surfaces, which in the case of the bracket can be observed in Figure 3a ( $N_d$ ), and in the case of the header, in Figure 3b ( $N_g$ ). The LBA only allows for analysis in which loads are treated as single parameter actions. Hence the relation between them is defined by coefficient  $\alpha$ , which is explained in equation (1).

$$\alpha = N_g / (N_g + N_d) \quad (1)$$

A detailed view of the approach to applying loads on a steel bracket is presented in Figure 3a, and to the header, in Figure 3b.

The size of the numerical issue, which is the number of nodes and finite elements, was different depending on

the parameters related to the geometry of the column. It depends on the distance between the external flange and the pointed lateral bracings  $h_z$ , as well as on their number  $m$ . Despite those slight differences, the number of finite elements for all of the models was approximate because it was around 52 thousand, and around 124 thousand in the case of the nodes.

### 3 Parametric analyses

#### 3.1 Programme of studies

The impact of the torsional restraint was examined in accordance with others factors, which are as follows: the longitudinal load distribution on the upper and lower segment of the column (expressed by  $\alpha$  – see eq. (1)), the number of lateral bracings and their distance to the column's external flange (defined by  $h_z$ ). It was assumed that a critical load  $N_{cr}$  is defined as a vertical support reaction, which is the sum of the applied external loads ( $N_g + N_d$ ). The sets and the nomenclature of the numerical models created in such a way are presented in Table 1. The description of particular numerical models depends on the type of the analysed parameter and is generally described by seven digits (xxxx-xxx) separated by a hyphen. The first digit describes the appropriate number of lateral restraints, the second informs whether the bracket is torsionally restrained and the third and

fourth fold up to the number of the load case that refers to the  $\alpha$  parameter. The last three digits after the hyphen are the distances between the lateral restraints and the column's external flange expressed by  $h_z$  in millimetres.

In each series, 21 models were analysed, assuming that the step for the  $\alpha$  parameter is at every 0.05. It means that in the case of series xx01-xxx, its value is equal to  $\alpha = 1.00$  (which stands only for the action applied to the header  $N_g$ ), for series xx02-xxx –  $\alpha = 0.95$ , and so on up to series xx21-xxx for which  $\alpha = 0.00$  (which stands only for the action applied to bracket  $N_d$ ).

Six different distances between the lateral restraints and external flange  $h_z$  were taken into consideration: 8, 32, 56, 80, 104 and 128 mm.

The number of lateral restraints was also varied. Five different schemes with total restraint numbers  $m$  equal to 1, 2, 4, 6, and 8 were taken into consideration. All the examples are presented in Figure 4. The main aim of this diversification was to determine the minimal number of bracings that impose the columns prescribed axis of rotation.

The buckling procedure implemented in the Abaqus FEA software allows both eigenvectors and eigenvalues to be obtained. The second term should be understood as the multiplier of the considered load case, which is usually denoted as  $a_{cr}$ . Hence the critical load  $N_{cr}$  for the whole numerical model is bound with the multiplier using equation (2).

$$N_{cr} = \alpha_{cr} \cdot (N_g + N_d) \quad (2)$$

When summarizing the wide range of parametric studies, it should be noticed that one series was composed of 21 single numerical models (see Tab. 1). The whole number of analysed columns is a product of the numbers of two types of bracket (with or without torsional restraint), the numbers of five types of pointed lateral bracings and the numbers of six different distances  $h_z$ . Altogether, the programme of the parametric study consisted of  $21 \cdot 2 \cdot 5 \cdot 6 = 1260$  individual numerical models.

### 3.2 Results

Such a great amount of data is difficult to process, and therefore the results are presented in graphical form. The data is depicted by using the Cartesian coordinate system in three-dimensional space. The abscissa ( $x$ -axis) presents the values of  $\alpha$  parameter, the ordinate ( $y$ -axis) illustrates the distances of the lateral restraint from the external flange of the column  $h_z$ , and the applicate ( $z$ -axis) shows the values of critical loads  $N_{cr}$ . Such a representation creates what is known as a stability surface, which can be shown as a 3D plot (see Fig. 5) or contour map (see Fig. 6). This kind of presentation allows for an easy analysis and comparison of results in a simple way. More detailed outcomes can be obtained by creating cutting planes through the stability surfaces.

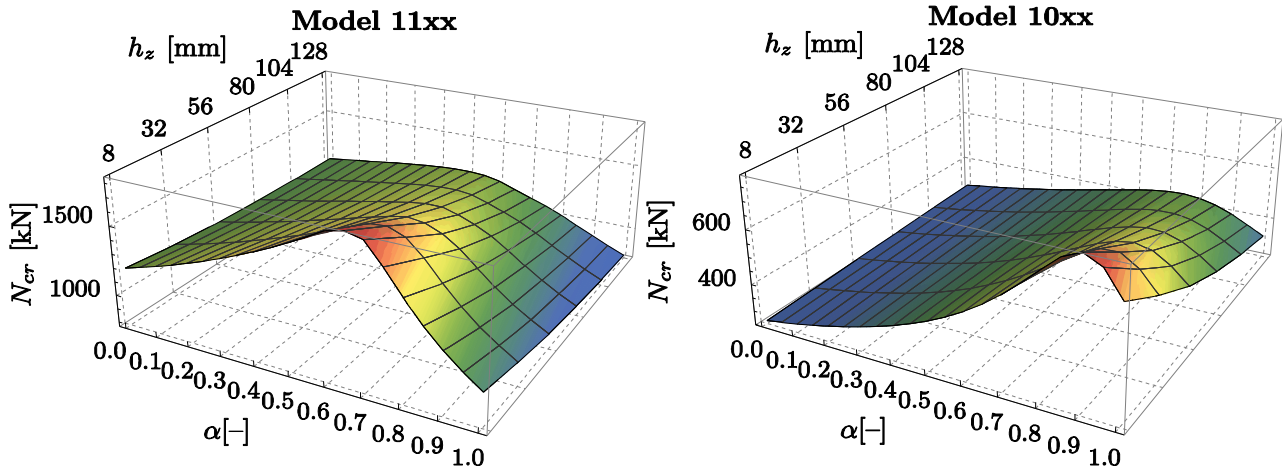


Fig. 5. Graphical presentation of critical forces  $N_{cr}$  of columns with (11xx) and without torsional restraint (10xx) shown as a 3D plot.

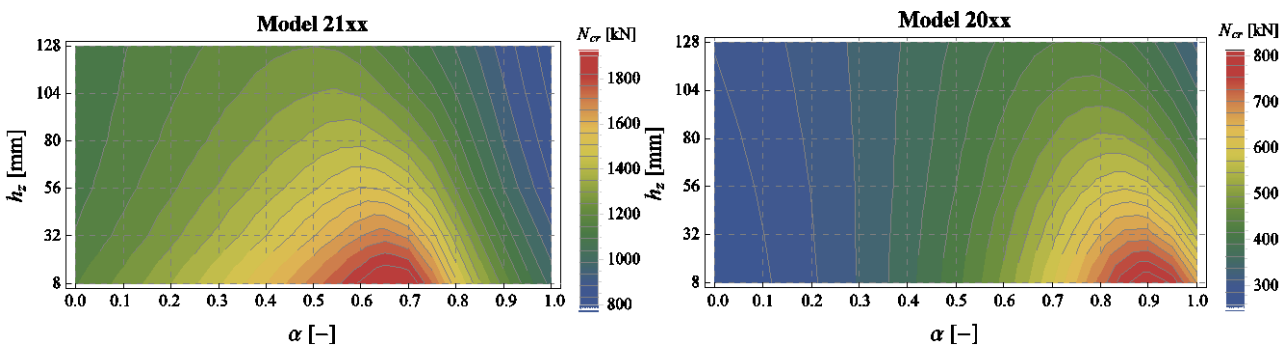
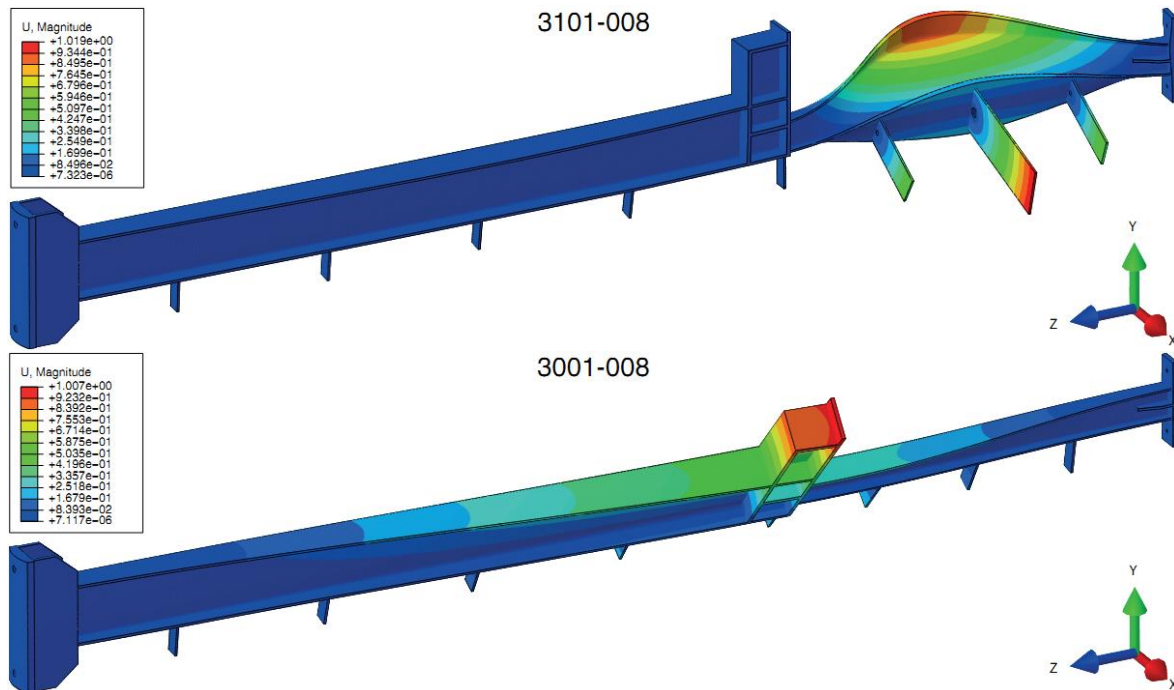


Fig. 6. Graphical presentation of critical forces  $N_{cr}$  of columns with (21xx) and without torsional restraint (21xx) shown as a contour map.



**Fig. 7.** Eigenforms of the numerical model series 3101-008 (with torsional restraint) and 3001-008 (without torsional restraint).

By cutting the abscissa or the ordinate by the vertical plane, it is possible to compare and evaluate the influence of one of the parameters ( $\alpha$  or  $h_2$ ) on a simple chart.

### 3.2.1 Influence of the torsional restraint

The torsional restraint is the most significant factor with the biggest impact on critical loads  $N_{cr}$ . It is clearly visible in Figure 5, which shows the results for a set of columns with four lateral restraints ( $m = 4$ ) along its external flange (see Fig. 4) with (11xx) or without additional torsional restraint (10xx) of the bracket.

The analysis of all the sets of data leads us to the conclusion that this procedure significantly increases critical loads  $N_{cr}$ . It is worth noting that on average those values advanced twofold (or in some cases even tripled).

The reason for this can be put down to the torsional restraint that enforces the new shape of the eigenforms, which can be observed in Figure 7. The numerical model denoted 3001-008, which stands for an element with eight lateral restraints located 8 mm from the external flange without torsional restraint and loaded only by action  $N_g$  applied to the header ( $\alpha = 1.00$ ), loses its spatial stability due to the occurrence of flexural-torsional buckling for both segments of the column. In this case the critical cross-section is located above the abrupt change of its stiffness (above the bracket). Application of the bracket's torsional restraint (see model 3101-008 in Fig. 7) also triggers off flexural-torsional buckling, but in this case it is limited only to the upper segment.

Interesting conclusions can also be drawn from the plots presented in Figures 5 and 6. We can observe that the profiles of surfaces with and without torsional

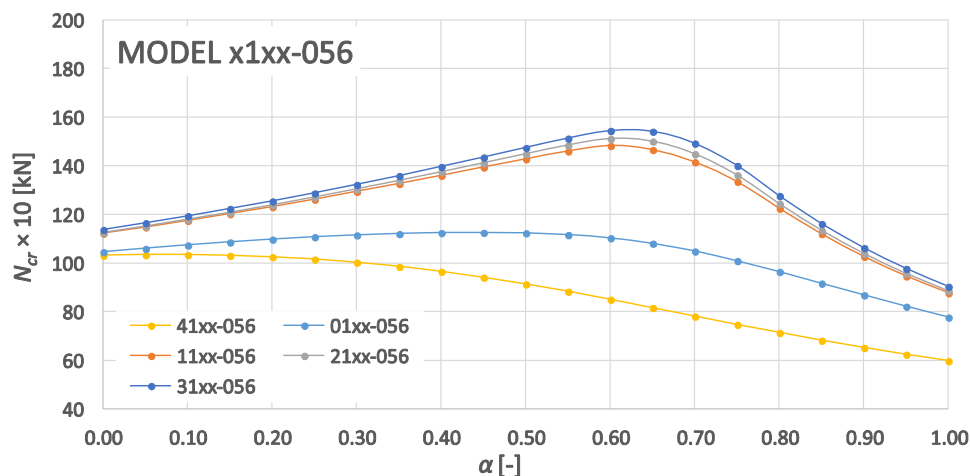


**Fig. 8.** Comparison of critical loads  $N_{cr}$  of numerical model series x1xx-056.

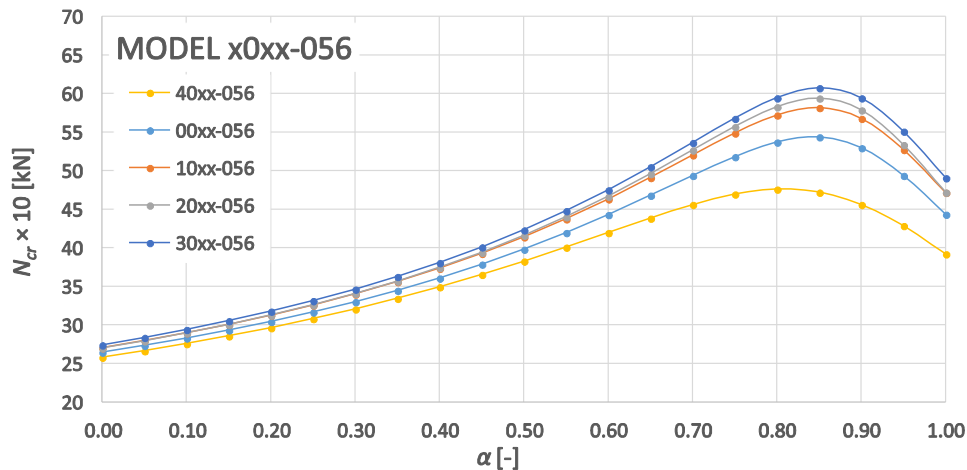


**Fig. 9.** Comparison of critical loads  $N_{cr}$  of the numerical model series x0xx-056.

restraint are diversified. Common for both of them is the characteristic peak value, but its location is not the same. For elements without torsional restraint, it appears when the range of the  $\alpha$  parameter reaches values between 0.8 and 0.9 close to the smallest value of  $h_z$ , which is 8 mm. Columns with torsional restraints reach such a peak when the  $\alpha$  ratio is smaller and takes values between 0.6 and 0.7. This can be particularly noticed on the contour maps shown in Figure 6. The above remarks can obviously not be applied to all steel stepped columns because it is strictly correlated to its geometry, particularly to the eccentricities between the axis of the upper and lower segments, as well as the bracket span.

The critical load  $N_{cr}$  is a concatenated dependency on which, beyond the above-mentioned eccentricities, external actions apply. It creates a complex distribution of internal forces because the lower, as well as upper segments, are loaded by bending moments with different signs. It means that there is a certain configuration of loads (expressed by  $\alpha$ ), in which both segments are not bent, but only compressed. For this particular column, it occurs when  $\alpha$  is equal to 0.85 [9].

### 3.2.2 Influence of the number of lateral restraints

The number of lateral restraints  $m$  is a parameter that has an impact on critical loads  $N_{cr}$  and on the shape of eigenforms. However, it is strongly related to other parameters, such as the distance between restraints and the column external flange  $h_z$ , and also the  $\alpha$  ratio that defines the relation between the two external actions  $N_g$  and  $N_d$ .

An exemplary impact of the number of lateral restraints  $m$  is presented in Figure 8. This chart was created by cutting several stability surfaces that were plotted for several series of numerical models with a different number of lateral restraints and with additional torsional restraint. A similar profile, but with smaller values of  $N_{cr}$ , was obtained for elements without torsional restraint. It is possible to observe that the  $m$  number depends on the  $\alpha$  ratio and that it is the most influential for values ranging from 0.2 to 1.0. The reason

for this is the fact that for small values of  $\alpha$ , the lower segment of the column is loaded by a greater bending moment, which compresses the internal flange that is not laterally restrained. The most appealing conclusion from the analyses of the influence of the number of lateral restraints is the fact that there is a limited number of them. However, this is sufficient from a practical point of view. The highest last three curves presented in Figure 8 are almost overlapping. This leads to the conclusion that in this case columns with four ( $m = 4$ ) pointed lateral bracings achieve the same critical capacity as columns with a bigger number of lateral restraints. This also means that the analytical model for such elements may be simplified to a model of a column with a prescribed axis of rotation [8-9]. Therefore, further increasing the number  $m$  of lateral restraints is pointless. The biggest difference in critical loads does not exceed 6%. It should be noted that the above observations refer to columns with an approximately equal spacing between restraints and also to those with restraints applied to both segments of the elements.

### 3.2.3 Influence of the external loads

The influence of the external loads is expressed by the  $\alpha$  parameter, which was already explained using equation (1). It is not an independent factor because it is coupled with other coefficients. Two of them have the biggest impact on shaping the characteristics of the  $\alpha$  parameter: a lack of proper torsional restraint of the bracket and the distance of lateral restraint to the external flange of column  $h_z$ . The influence is strictly related to the shape of the eigenforms. If they are similar, the shapes of the charts or surfaces are also similar. When additional restraints enforce different types of eigenforms, the corresponding charts are also different.

It was generally observed that in the case of laterally restrained steel I-columns with a single stepped asymmetric change of cross-section, the critical load  $N_{cr}$  can be divided into two phases. The first one is a phase of increase, and the second is a phase of decrease. What is different for columns with and without torsional restraint is that two cases reach peaks for different  $\alpha$

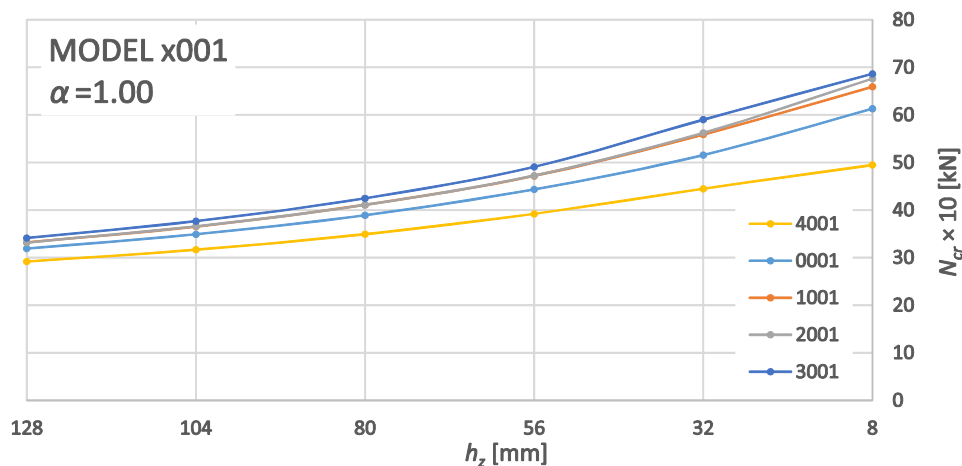


**Fig. 10.** Comparison of critical loads  $N_{cr}$  of the numerical model series x001-xxx.

ratios. Torsionally unrestrained columns achieve the highest values of critical forces  $N_{cr}$  when the  $\alpha$  ratio ranges between 0.8 and 0.9. For torsionally restrained elements, it is between 0.6 and 0.7. It is strongly coupled with the distribution of internal forces, which has already been mentioned.

### 3.2.4 Influence of the location of lateral restraint

The influence of the distance between lateral restraint and the column's external flange is only significant in certain cases. Possible torsional restraint of the bracket and  $\alpha$  ratio might be additional factors, which are considered together.

The  $\alpha$  ratio is only relevant when it achieves values greater than 0.5. Otherwise, the lower segment of the column is eccentrically loaded. In such a case, the biggest compression stresses occur in the internal unbraced flange, and therefore restraining the external flange becomes insufficient.

The influence of the location of lateral restraint can be evaluated by the assumption that other factors are constant. It is presented in Figure 10. This chart was made by creating a section through the many stability surfaces (one of them is presented in Fig. 5). On the example of the column without torsional restraint, it can be noticed that the farther the distance  $h_z$  is, the smaller the obtained value of critical load  $N_{cr}$ . The increase of such a distance up to infinity implies the asymptotic value that can be obtained for a laterally unrestrained column. In this example the smallest value of  $h_z$  causes a 50% increase of the critical load. Smaller benefits are observed for elements with torsional restraint, which is because they reach up to 20%. What became characteristic for these types of columns is that elements with the smallest number of lateral restraints, which are 41xx and 01xx, turned out to be insensitive on a differentiation of  $h_z$  distance. Both types buckle in flexural-torsional form, but with domination of flexural buckling. In the series with only one lateral restraint (41xx), one sine wave on both segments can be observed. On the upper segments of elements with three

lateral restraints (01xx), only a half sine wave can be observed.

Contour maps are very convenient when evaluating the influence of distance  $h_z$  on critical load  $N_{cr}$  (see Fig. 6). The shape and distribution of the contour lines directly indicates its impact. For the series with six lateral restraints without torsional restraint (see model 20xx in Fig. 6), it is evident when the  $\alpha$  ratio reaches values between 0.0 and 0.55. The contour lines are almost vertical, which indicates that the location of lateral bracings has no meaning from a practical point of view. The main reason for this is the already mentioned load eccentricity, which causes the biggest compression stresses in the internal flange. The location of lateral restraints is more influential when the  $\alpha$  parameter is bigger than 0.6 or when torsional restraint is applied.

## 4 Conclusions

The paper presents the results of a set of numerical investigations on the critical load capacity of steel I-columns with single stepped asymmetric change in their cross-section. The appropriate finite element method models were developed to evaluate the influence of: the torsional restraint of the bracket, the relation between external loads, the number of lateral restraints and its distance to the external flange.

The wide parametric analysis revealed that single torsional restraint has a significant impact on elastic critical loads. In some situations, which are coupled with other factors, the application of torsional restraint can even triple the value of the critical load. It is comparable, but maybe not in such a range, to the number of lateral restraints. The analysis showed that by increasing its number, it is possible to increase the critical load. However, the efficiency of this theory is limited by a certain number of lateral restraints. Increasing it further is pointless and not beneficial because it enforces its prescribed axis of rotation.

Calculations were carried out using resources provided by Wrocław Centre for Networking and Supercomputing (<http://wcss.pl>), grant No. 228.

## References

1. AISC, *Guide for the Design and Construction of Mill Buildings*, Association of Iron and Steel Engineers (2003)
2. W. Kucharczuk, S. Labocha, *Hale o konstrukcji stalowej. Poradnik projektanta* (Polskie Wydawnictwo Techniczne, Rzeszów, 2012) (in Polish)
3. J. D. Aristizabal-Ochoa, Stability and minimum bracing for stepped columns with semirigid connections: Classical elastic approach, *Structural Engineering and Mechanics*, **5**, p. 415–431 (1997).
4. A. M. Girão Coelho, P. D. Simão, F. S. K. Bijlaard, Stability design criteria for steel column splices, *Journal of Constructional Steel Research*, **66**, p. 1261–1277 (2010)
5. B. Gosowski, Spatial buckling of thin-walled steel-construction beam-columns with discrete bracings, *Journal of Constructional Steel Research*, **52**, p. 293–317 (1999)
6. B. Gosowski, Spatial stability of braced thin-walled members of steel structures, *Journal of Constructional Steel Research*, **59**, p. 839–865 (2003)
7. B. Gosowski, Zur Stabilitätsanalyse der axial belasteten Stahlbaustützen mit I-Querschnitt, *Bauingenieur*, **63**, p. 229–237 (1988)
8. B. Gosowski, Drillknicken einfach-symmetrischer Stahlstützen mit erzwungener Drehachse. *Stahlbau*, **77**, p. 669–680 (2008)
9. M. Redecki, *Load bearing capacity of laterally restrained steel I-columns with single stepped asymmetric change of cross-section*, Raporty Wydziału Budownictwa Lądowego i Wodnego Politechniki Wrocławskiej, Ser. PRE; nr 4/2017. (in Polish)
10. Abaqus FEA 6.14, Abaqus FEA Documentation, Dassault Systèmes 2014